Eur. Phys. J. B **39**, 377–384 (2004)
DOI: 10.1140/epjb/e2004-00203-1

THE EUROPEAN PHYSICAL JOURNAL B

Orientation dependence of proximity effect in ferromagnet/d-wave superconductor junctions

L.Y. Yang, Z.M. Zheng, H.L. Yu, G.Y. Sun, and D.Y. Xing[a]

National Laboratory of Solid State Microstructures and Department of Physics, Nanjing University, Nanjing 210093, P.R. China

Received 26 November 2003 / Received in final form 10 February 2004
Published online 12 July 2004 –

Abstract. The Nambu spinor Green's function approach is applied to studying the proximity effect in ferromagnet/d-wave superconductor (FM/d-wave SC) junctions. It is found that the magnitude of the proximity effect depends to a great extent on the orientation of the SC crystal with respect to the interface normal. On the FM side, near the interface there are two different types of density of states (DOS) with superconducting features. On the SC side, the DOS near the interface is spin dependent, indicating a local coexistence of weak ferromagnetism and d-wave superconductivity.

PACS. 74.45.+c Proximity effects; Andreev effect; SN and SNS junctions – 74.50.+r Tunneling phenomena; point contacts, weak links, Josephson effects – 74.20.Rp Pairing symmetries (other than s-wave)

1 Introduction

Proximity effects in ferromagnet/superconductor (FM/SC) structures have recently attracted much attention in experimental and theoretical investigations [1–23]. Cooper pairs injected from SC to FM are not broken immediately and can survive for a time corresponding to a traveled length of the order of ξ_F, giving rise to a superconducting order parameter in the FM near the interface, where $\xi_F = \hbar v_F/2h_0$ is the coherent length in FM with v_F the Fermi velocity and $2h_0$ the exchange energy, equal to the difference in energy between spin-up and spin-down bands. On the other hand, the injection of spin-polarized electrons from the FM into the SC leads to a stronger pair-breaking effect than in a normal-metal/SC (NM/SC) structure. In SC near the FM/SC interface there may appear gapless superconductivity [19] in addition to the decrease of superconducting order parameter. The Andreev reflection (AR) process [24] plays an important role in the proximity effect. In this process an electron in the FM is reflected from the FM/SC interface as a hole along an approximately time-reversed path, where the time-reverse symmetry has been broken by the presence of the FM. The inducement of superconductivity in the FM and its suppression in the SC may be attributed to the coherent coupling of electrons and holes in FM and a pair-breaking effect in SC, respectively, both produced by the AR process.

In a recent work on the proximity effect in FM/SC junctions, Kontos et al. [10] measured tunnelling spectra of $Al/Al_2O_3/PdNi/Nb$ tunnel junctions where PdNi is a ferromagnetic alloy and Nb is an s-wave SC. The tunneling spectra they measured corresponds to the density of states (DOS) in PdNi at the Al_2O_3/PdNi interface, exhibiting an Nb-induced superconducting feature and a change from "0" to "π" state with increasing thickness of the PdNi layer. Zareyan et al. [11] and Sun et al. [19] studied theoretically the proximity effect in the FM/s-wave SC junction. The DOS in FM was reproduced with the superconducting feature of the "0" and "π" states [11,19], and the gapless superconductivity was obtained in the s-wave SC near the FM/SC interface [19]. It is expected that similar characteristics of the proximity effect just described also exist in the FM/d-wave SC junctions. In addition, there must be effects particular to them, unlike in the FM/s-wave SC junctions.

Since the cuprate superconductors with high critical temperature were identified as having a $d_{x^2-y^2}$-wave symmetry of pair potential, the study of FM/d-wave junctions has become an important topic. The pair potential for $d_{x^2-y^2}$-wave symmetry has $\cos 2\theta$ dependence, resulting in a number of interesting phenomena. For example, for {110}-orientation, the amplitude of the pair potential disappears for $\theta = \pi/4$. In this case, the d-wave symmetry could lead to a sizable areal density of midgap states [25], which is the origin of the zero-bias conductance peak observed in most high-T_c superconductor junctions. This feature can be used as a clear signature to distinguish between d-wave and anisotropic s-wave

[a] e-mail: dyxing@nju.edu.cn

superconductors [25]. The conductance spectra for charge and spin currents have been calculated theoretically in the FM/d-wave SC junctions [5,6]. The zero-bias conductance peaks were obtained for the [110] interface, which are close to the local DOS in the d-wave SC at the interface. Very recently, Stefanakis and Melin [26] have studied the proximity effect in FM/SC hybrid structures using the Bogoliubov-de Gennes (BdG) formalism within a two-dimension (2D) extended Hubbard model and made a comparison between s-wave and d-wave pairing cases. In the d-wave case, the proximity effect depends on the orientation of the SC crystal with respect to the interface normal. For the c-axis parallel to the interface normal, the FM/d-wave SC junction is a 3D system; while for the c-axis along a direction within the interface, it may be regarded as a 2D system. In the latter case, the angle between the a-axis and the interface normal also plays an important role in the proximity effect. Such an orientation dependence of the proximity effect is one of motivations of this study.

Another interesting topic is the possible coexistence of ferromagnetism and spin-singlet superconductivity [27]. Since both of them have different requirements for spin orientation of itinerant electrons, it is very difficult for them to coexist in a bulk sample. It was shown [28] that their coexistence condition in the d-wave case is given by $h_0/\Delta_0 < 0.56$ for zero center-of-momentum Cooper pairs and $0.56 < h_0/\Delta_0 < 1.06$ for the FFLO states [29,30] for the Cooper pair having a finite center-of-mass momentum $Q = 2h_0/\hbar v_F$, where Δ_0 is the maximum energy gap at $T = 0$. However, h_0 in a bulk FM is typically at least 2 orders of magnitude larger than Δ_0 of a bulk SC. Until recently, whether or not the itinerant ferromagnetism can coexist with spin-singlet superconductivity is still under dispute [31–33]. On the experimental side, the coexistence of ferromagnetism and superconductivity was reported in Cu-rich lanthanum Cu-oxides [34] and in c-axis oriented $YBa_2Cu_3O_7/La_{0.67}Ba_{0.33}MnO_3$ superlattices [35]. As a result, it is highly desirable to study probable coexistence between ferromagnetism and superconductivity near the FM/SC interface, which is another motivation for this work.

In this paper, we extend the theoretical approach of Blonder-Tinkham-Klapwijk (BTK) [36], which was previously used to calculate differential conductance of an NM/s-wave SC junction, to study the proximity effect in FM/d-wave SC junctions, from which wave functions of quasiparticles on both FM and SC sides can be obtained. We then present a formulation of the Green function in 2D and 3D junction structures by extending McMillan's formula [37] originally developed for a 1D s-wave superconductor. The superconducting order parameter is described by the imaginary part of the off-diagonal component of the Green's function, and the density of states (DOS) is proportional to the imaginary part of its diagonal component. It is found that the spatial changes of the superconducting order parameter and DOS due to the proximity effect depend to a great extent on the orientation of the d-wave SC crystal with respect to the interface normal. On the FM side, there are two types of DOS with d-wave superconducting features; while on the SC side, there exists a local coexistence between weak ferromagnetism and d-wave superconductivity near the interface.

2 Model and theory

Consider an FM/d-wave SC junction structure of semi-infinite FM and SC separated by a very thin insulating layer located at $x = 0$. If the c-axis of the d-wave SC is along a direction within plane $x = 0$, which is taken to be the z-axis, such an FM/d-wave SC junction may be regarded as a two-dimensional system. The FM is described by an effective single-particle Hamiltonian with exchange energy h_0, the d-wave SC is described by a BCS-like Hamiltonian, and the insulating layer described by a δ-type barrier potential $V(x) = U\delta(x)$ where U depends on the product of barrier height and width. For simplicity, the effective masses m are taken to be equal in both FM and SC. The d-wave pair potential is a function of angle θ_S between the quasiparticle wavevector and the interface normal and given by $\Delta(x) = \Delta^d_{\pm} = \Delta_0 \cos(2\theta_S \mp 2\alpha)$ for $x > 0$, where Δ^d_+ (Δ^d_-) stands for the pair potential for electron-like (hole-like) quasiparticles [13], Δ_0 is a constant, and α is the angle between the a-axis of the crystal and the interface normal. $\alpha = \pi/4$ for the interface normal along the [110] orientation and $\alpha = 0$ for the interface normal along [100] orientation. $\Delta(x) = 0$ in the FM region for $x < 0$. It is worth noting that the effective pair potentials experienced by the electron-like and hole-like quasiparticles in the d-wave SC are usually different and may even have opposite signs under certain circumstances.

We adopt the BdG approach [38] to study the FM/d-wave SC junction. This approach has been widely applied to describing quasiparticle states in superconductors with spatially varying pair potential. In the FM/SC junction, the quasiparticle states are generally expressed by a four-component wave function, respectively, for electron-like quasiparticle (ELQ) and hole-like quasiparticle (HLQ) with spin up and down. In the absence of spin-flip scattering, the four-component BdG equations may be decoupled into two sets of two-component equations: one for the spin-up electron-like and spin-down hole-like quasiparticle wave function ($u_\uparrow$, $v_\downarrow$), the other for $u_\downarrow$ and $v_\uparrow$. The BdG equation is given by

$$\begin{bmatrix} H_0(\mathbf{r}) - \eta_\sigma h(\mathbf{r}) & \Delta(x,\theta) \\ \Delta^*(x,\theta) & -H_0(\mathbf{r}) - \eta_\sigma h(\mathbf{r}) \end{bmatrix} \begin{bmatrix} u_\sigma(x,\theta) \\ v_{\bar\sigma}(x,\theta) \end{bmatrix} = E \begin{bmatrix} u_\sigma(x,\theta) \\ v_{\bar\sigma}(x,\theta) \end{bmatrix}. \quad (1)$$

Here $H_0(\mathbf{r}) = -\hbar^2\nabla_r^2/2m + V(\mathbf{r}) - E_F$ with $V(\mathbf{r})$ the usual static potential, E is the quasiparticle energy relative to the Fermi energy E_F. $h(\mathbf{r}) = h_0\Theta(-x)$ with h_0 the exchange energy in FM and $\Theta(-x)$ the unit step function, $\eta_\sigma = 1$ for $\sigma = \uparrow$ and -1 for $\sigma = \downarrow$, and $\bar\sigma$ stands for

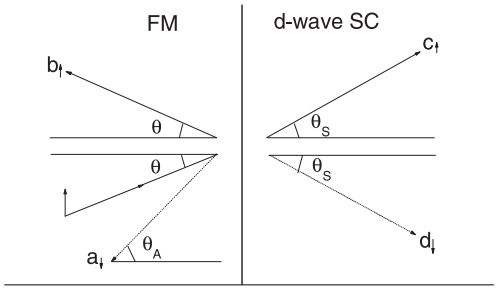

Fig. 1. Schematic illustration of the reflection and transmission processes at the FM/d-wave SC interface.

the spin opposite to σ. Following McMillan's method [37], we employ two envelop functions that are smooth on the atomic scale length, $u_\sigma(\mathbf{r}) = \bar{u}_\sigma(\mathbf{r})\exp(i\mathbf{k}_\mathbf{F}^\sigma \cdot \mathbf{r})$ and $v_{\bar\sigma}(\mathbf{r}) = \bar{v}_{\bar\sigma}(\mathbf{r})\exp(i\mathbf{k}_\mathbf{F}^{\bar\sigma}\cdot\mathbf{r})$. By neglecting the terms as $\partial^2/\partial x^2$ which are of order Δ_0/E_F with respect to the $\partial/\partial x$ term, we obtain the reduced BdG equations for the quasiparticle wave functions

$$\frac{-i\hbar^2 k_F^\sigma}{m}(\hat{\mathbf{k}}\cdot\nabla)\bar{u}_\sigma(\mathbf{r}) + \bar{\Delta}^*(\mathbf{r})\bar{v}_{\bar\sigma}(\mathbf{r}) = E\bar{u}_\sigma(\mathbf{r}), \quad (2)$$

$$\frac{i\hbar^2 k_F^{\bar\sigma}}{m}(\hat{\mathbf{k}}\cdot\nabla)\bar{v}_{\bar\sigma}(\mathbf{r}) + \bar{\Delta}(\mathbf{r})\bar{u}_\sigma(\mathbf{r}) = E\bar{v}_{\bar\sigma}(\mathbf{r}), \quad (3)$$

where $\bar{\Delta}(\mathbf{r}) = \Delta(\mathbf{r})\exp[i(\mathbf{k}_\mathbf{F}^\sigma - \mathbf{k}_\mathbf{F}^{\bar\sigma})\cdot\mathbf{r}]$, $k_F^\sigma = k_F\sqrt{1+\eta_\sigma h_0/E_F}$ is the spin-dependent Fermi wavevector in FM with k_F the Fermi wavevector in SC, and $\hat{\mathbf{k}}$ is a unit vector denoting the direction of wavevector $\mathbf{k}$. At the FM/SC interface there are four types of quasiparticle injection process: electron and hole injection from FM to SC, and ELQ and HLQ injection from SC to FM. Suppose a beam of spin-σ electrons incident on the interface at $x = 0$ at an angle θ from FM to SC. As shown in Figure 1, there are four possible trajectories: normal reflection (NR) b_1^σ at angle θ and Andreev reflection [24] (AR) $a_1^{\bar\sigma}$ as a hole with spin-$\bar\sigma$ at angle θ_A in FM, and transmission c_1^σ and $d_1^{\bar\sigma}$ to SC at angle θ_S, respectively, as a spin-σ ELQ and a spin-$\bar\sigma$ HLQ.

It is worth pointing out that the AR coefficient $a_1^{\bar\sigma}$ is labeled with $\bar\sigma$ because the AR results in an electron deficiency in the spin-$\bar\sigma$ subband of the FM, even though it is at times called a spin-σ hole. With general solutions of the BdG equations, the wave functions in FM and SC regions can be obtained. Owing to translational invariance in the direction parallel to the interface, the wave functions in FM and SC are given by

$$\Psi_{1\sigma}^{FM} = \begin{pmatrix}1\\0\end{pmatrix}e^{iq_e^\sigma x\cos\theta} + a_1^{\bar\sigma}\begin{pmatrix}0\\1\end{pmatrix}e^{iq_h^{\bar\sigma}x\cos\theta_A} + b_1^\sigma\begin{pmatrix}1\\0\end{pmatrix}e^{-iq_e^\sigma x\cos\theta} \quad (4)$$

for $x < 0$, and

$$\Psi_{1\sigma}^{SC} = c_1^\sigma\begin{pmatrix}u_+^d e^{i\phi_+^d}\\ v_+^d\end{pmatrix}e^{ik_+^d x\cos\theta_S} + d_1^{\bar\sigma}\begin{pmatrix}v_-^d e^{i\phi_-^d}\\ u_-^d\end{pmatrix}e^{-ik_-^d x\cos\theta_S} \quad (5)$$

for $x > 0$. Here $q_e^\sigma\cos\theta = k_F^\sigma\cos\theta + mE/(\hbar^2 k_F^\sigma\cos\theta)$ and $q_h^\sigma\cos\theta_A = k_F^\sigma\cos\theta_A - mE/(\hbar^2 k_F^\sigma\cos\theta_A)$, indicating different Fermi wavevector components perpendicular to the interface for the spin-σ electrons and holes in FM. In SC, $k_\pm^d\cos\theta_S = k_F\cos\theta_S \pm m\sqrt{E^2 - |\Delta_\pm^d|^2}/(\hbar^2 k_F\cos\theta_S)$ and $\tilde{k}_\pm^d\cos\theta_S = k_F\cos\theta_S \mp m\sqrt{E^2 - |\Delta_\pm^d|^2}/(\hbar^2 k_F\cos\theta_S)$ with $k_F = \sqrt{2mE_F}/\hbar$. In equation (5), $(u_\pm^d)^2 = 1 - (v_\pm^d)^2 = (1 + \sqrt{1 - |\Delta_\pm^d/E|^2})/2$, and $\phi_\pm^d = \cos^{-1}[\cos 2(\theta_S \mp\alpha)/|\cos 2(\theta_S\mp\alpha)|]$. In the BTK approach, since the wave-vector component parallel to the interface is assumed to remain unchanged in reflection and transmission, i.e., $k_F^\sigma\sin\theta = k_F^{\bar\sigma}\sin\theta_A = k_F\sin\theta_S$, the angles θ, θ_A and θ_S differ from each other except when $\theta = 0$. For example, for the incident electrons with spin up, we have $k_F^\uparrow > k_F > k_F^\downarrow$, so that $\theta < \theta_S < \theta_A$. With increasing θ, both θ_A and θ_S become large. As θ exceeds $\sin^{-1}(k_F^\downarrow/k_F^\uparrow)$, the x component of the wavevector in the AR process, $\sqrt{{k_F^\downarrow}^2 - {k_F^\uparrow}^2\sin^2\theta}$, will become purely imaginary and the Andreev reflected quasiparticles do not propagate, which is called the virtual AR.

As θ is further increased to be $\theta > \sin^{-1}(k_F/k_F^\uparrow)$, the transmitted quasiparticles do not propagate and so the net charge current from FM to SC vanishes. All the coefficients $a_1^{\bar\sigma}$, b_1^σ, c_1^σ and $d_1^{\bar\sigma}$ can be determined by matching the boundary conditions at $x = 0$: $\Psi_{1\sigma}^{FM}(0) = \Psi_{1\sigma}^{SC}(0)$ and $(d\Psi_1^{SC}/dx)_{x=0} - (d\Psi_1^{FM}/dx)_{x=0} = 2k_F\cos\theta Z\Psi_1^{FM}(0)$ where $Z = mU/k_F\cos\theta$ represents the strength of the interfacial barrier. The wave functions for the other three types of quasiparticle injection processes can be obtained in a similar way.

The next step is to construct the Nambu spinor Green's function in the FM/d-wave SC structure. With the wave functions $\Psi_{i\sigma}(i = 1,2,3,4$ and $\sigma =\uparrow,\downarrow)$, the retarded Green's function [9,16,39,40] is given by

$$G_r^\sigma(x,x',E) = \begin{cases}\alpha_1^\sigma\Psi_{3\sigma}(x)\Psi_{1\sigma}^t(x') + \alpha_2^\sigma\Psi_{3\sigma}(x)\Psi_{2\sigma}^t(x') \\ +\alpha_3^\sigma\Psi_{4\sigma}(x)\Psi_{1\sigma}^t(x') + \alpha_4^\sigma\Psi_{4\sigma}(x)\Psi_{2\sigma}^t(x'), \\ \qquad x \le x' \\ \beta_1^\sigma\Psi_{1\sigma}(x)\Psi_{3\sigma}^t(x') + \beta_2^\sigma\Psi_{1\sigma}(x)\Psi_{4\sigma}^t(x') \\ +\beta_3^\sigma\Psi_{2\sigma}(x)\Psi_{3\sigma}^t(x') + \beta_4^\sigma\Psi_{2\sigma}(x)\Psi_{4\sigma}^t(x'), \\ \qquad x \ge x'\end{cases} \quad (6)$$

where the wave function $\Psi_{i\sigma}^t(x)$ is the transposition of $\Psi_{i\sigma}(x)$. The coefficients α_i^σ and $\beta_i^\sigma(i = 1,2,3,4)$, can be determined by satisfying the following boundary conditions: $G_r^\sigma(x, x+0_+, E) = G_r^\sigma(x, x-0_+, E)$, and $dG_r^\sigma(x,x',E)/dx|_{x=x'+0_+} - dG_r^\sigma(x,x',E)/dx|_{x=x'-0_+} = (2m/\hbar^2)\hat{\tau}_3$ with $\hat{\tau}_3$ the Pauli matrix. After carrying out a little tedious calculation, we get diagonal and off-diagonal

components of the 2×2 retarded Green's functions as

$$[G_r^\sigma(x,x,\theta,E)]_{11} = -\frac{im}{\hbar^2 q_e^\sigma \cos\theta}\left(1 + b_1^\sigma e^{-2iq_e^\sigma x\cos\theta}\right), \tag{7}$$

$$[G_r^\sigma(x,x,\theta,E)]_{12} = -\frac{im}{\hbar^2 q_h^{\bar\sigma}\cos\theta_A} a_2^\sigma e^{i\left(q_h^{\bar\sigma}\cos\theta_A - q_e^\sigma\cos\theta\right)x}, \tag{8}$$

in FM, and

$$\begin{aligned}[G_r^\sigma(x,x,\theta_S,E)]_{11} &= -\frac{imE}{\hbar^2 k_+^d \Omega_+\cos\theta_S} \\ &\times\Big[e^{i\left(k_+^d-\tilde k_-^d\right)x\cos\theta_S} u_+^d u_-^d e^{i\left(\phi_+^d+\phi_-^d\right)} + b_3^\sigma e^{2ik_+^d x\cos\theta_S}\left(u_+^d\right)^2 \\ &\quad + a_3^{\bar\sigma} e^{i\left(k_+^d-k_-^d\right)x\cos\theta_S} u_+^d v_-^d e^{i\left(\phi_+^d+\phi_-^d\right)}\Big] - \frac{imE}{\hbar^2 k_-^d \Omega_-\cos\theta_S} \\ &\times\Big[e^{i\left(\tilde k_+^d-k_-^d\right)x\cos\theta_S} v_+^d v_-^d e^{i\left(\phi_+^d+\phi_-^d\right)} + b_4^\sigma e^{-2ik_-^d x\cos\theta_S}\left(v_-^d\right)^2 \\ &\quad + a_4^{\bar\sigma} e^{i\left(k_+^d-k_-^d\right)x\cos\theta_S} u_+^d v_-^d e^{i\left(\phi_+^d+\phi_-^d\right)}\Big], \end{aligned} \tag{9}$$

$$\begin{aligned}[G_r^\sigma(x,x,\theta_S,E)]_{12} &= -\frac{imE}{\hbar^2 k_+^d \Omega_+\cos\theta_S} \\ &\times\Big[e^{i\left(k_+^d-\tilde k_-^d\right)x\cos\theta_S} u_-^d v_+^d e^{i\phi_-^d} + b_3^\sigma e^{2ik_+^d x\cos\theta_S} u_+^d v_+^d e^{i\phi_+^d} \\ &\quad + a_3^{\bar\sigma} e^{i\left(k_+^d-k_-^d\right)x\cos\theta_S} v_+^d v_-^d e^{i\phi_-^d}\Big] - \frac{imE}{\hbar^2 k_-^d \Omega_-\cos\theta_S} \\ &\times\Big[e^{i\left(\tilde k_+^d-k_-^d\right)x\cos\theta_S} u_-^d v_+^d e^{i\phi_+^d} + b_4^\sigma e^{-2ik_-^d x\cos\theta_S} u_-^d v_-^d e^{i\phi_-^d} \\ &\quad + a_4^{\bar\sigma} e^{i\left(k_+^d-k_-^d\right)x\cos\theta_S} u_+^d u_-^d e^{i\phi_+^d}\Big], \end{aligned} \tag{10}$$

in SC. Here $\Omega_\pm = \sqrt{E^2 - |\Delta_\pm^d|^2}$, and the expressions for the reflection and transmission coefficients are given in the Appendix.

From the Green's function obtained above, the local DOS of the quasiparticles, $N(x,E)$, and the superconducting order parameter, $F(x,\theta)$, can be calculated [40]. The local DOS of the quasiparticles is proportional to the imaginary part of the $[G_r^\sigma(x,x,\theta,E)]_{11}$,

$$N(x,E) = \frac{-1}{\pi}\sum_{\sigma,k_\parallel}\mathrm{Im}[G_r^\sigma(x,x,\theta,E)]_{11}, \tag{11}$$

where $k_\parallel = k\sin\theta$ is the parallel component of the momentum and the summation over $k_\parallel$ may be performed by the integral over θ. The superconducting order parameter $F(x)$ is determined by the off-diagonal component of the Green's function, $[G_r^\sigma(x,x,\theta,E)]_{12}$. In the s-wave case, the pair potential can be recalculated by $\Delta(x) = \lambda^* F(x)$ where λ^* is the effective electron-phonon coupling constant [37]. In the d-wave case, the attractive interaction $V(\mathbf{k}-\mathbf{k}')$ is proportional to $\cos(2\theta-2\alpha)\cos(2\theta'-2\alpha)$ [41], so that we have

$$\Delta(x,\theta) = \lambda^* F(x)\cos(2\theta-2\alpha), \tag{12}$$

with

$$F(x) = \frac{1}{\pi}\sum_{\sigma,k_\parallel'}\cos(2\theta'-2\alpha)\int_0^\infty dE\,\mathrm{Im}[G_r^\sigma(x,x,\theta',E)]_{12}. \tag{13}$$

If the c-axis of the d-wave SC is parallel to the interface normal (along the x-direction), the FM/d-wave SC junction needs to be considered as a three-dimensional (3D) system, in which $\Delta_0(x,\phi) = \Delta_0\cos(2\phi)$ for $x > 0$ at the beginning and $\Delta(x,\phi) = \Delta(x)\cos(2\phi)$ where ϕ is the angle between the a-axis of the crystal and the z direction. In this case, all the calculations can be performed in a similar way provided that all the wavevectors are taken to be 3D, and the summation in equations (11) and (13) are replaced by the integrals over θ and ϕ.

3 Results and discussions

In what follows we present and discuss numerical results from equations (11) and (13) together with equations (7–10). In Figure 2 we plot spatial variation of the amplitude of superconducting order parameters in the FM/d-wave SC structure for $\alpha = 0$ (solid line), $\alpha = \pi/4$ (dotted line), and the c-axis along the x-direction (dash-dotted line). On the FM side, there appears an oscillating superconducting order parameter induced by the proximity effect. As Cooper pairs are injected from SC to FM, the spin-σ ELQ and spin-$\bar\sigma$ HLQ interfere with each other, producing a damped oscillation of $F(x)$. Here $\xi_F = \hbar v_F/2h_0$ is the coherent length in FM, it is inversely proportional to the difference in the Fermi momentum between the spin-σ electron and spin-$\bar\sigma$ hole. Similar to the case of FM/s-wave SC junctions, the state with positive $F(x)$ is called the "0" state and that with negative $F(x)$ called the "π" state. They appear alternately with increasing distance from the FM/SC interface. On the SC side, the order parameter is diminished near the interface, which arises from the pair-breaking effect due to the injection of spin-polarized electrons from FM to SC. Here $\xi_S = \hbar v_F/2\Delta_0$ is the coherent length in SC, much longer than ξ_F. The proximity effect depends not only on the barrier strength, but also on the angle between the crystal axis and the interface normal, as shown in Figure 2. It is easily understood that the stronger the barrier strength, the weaker the proximity effect is.

The anisotropy dependence of the proximity effect is an interesting result. For the a-axis of SC crystal perpendicular to the interface ($\alpha = 0$), there is only a small decrease in $F(x)$, which is somewhat similar to the case of s-wave SC. For $\alpha = \pi/4$, however, $F(x)$ has a big decrease near the interface, even in the presence of large Z. This may stem from the fact that for $\alpha = \pi/4$, $\Delta = \Delta_0\sin 2\theta$ is an odd function of θ; while for $\alpha = 0$, $\Delta = \Delta_0\cos 2\theta$ is an even function of θ. The injection of spin-polarized electrons has a stronger pair-breaking effect on the former with a largest asymmetry with respect to the x-axis, along which a node appears in the order parameter of the bulk SC. Another difference in $F(x)$ between $\alpha = 0$ and

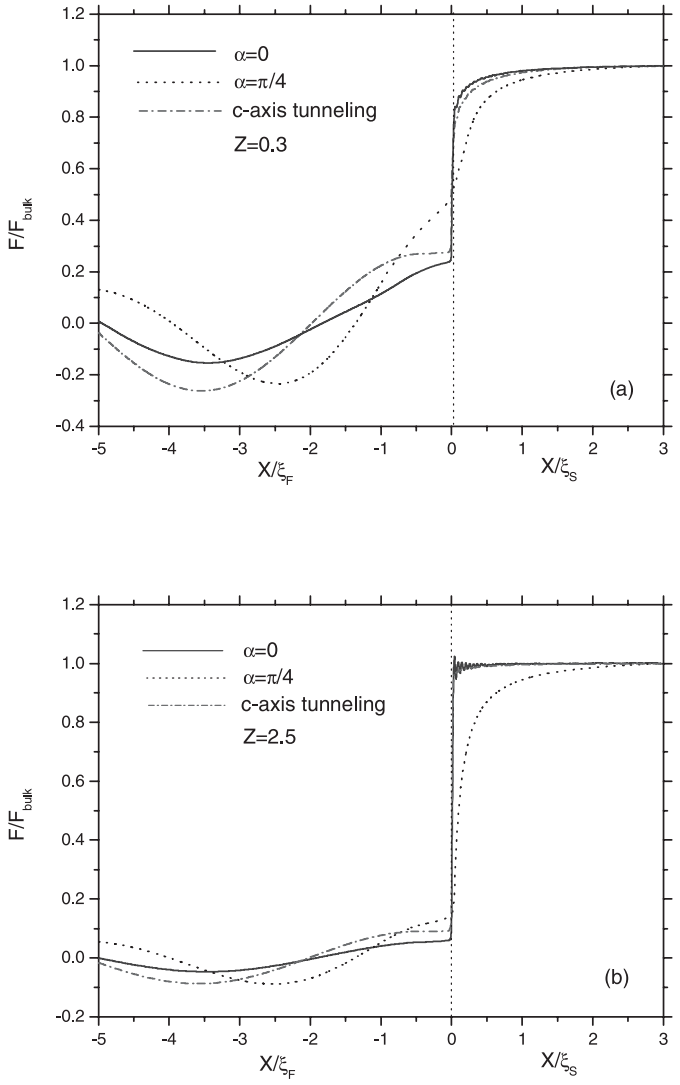

Fig. 2. Spatial change of the superconducting order parameter in FM/d-wave SC junctions for $Z = 0.3$ (a) and $Z = 2.5$ (b) with $\alpha = 0$ (solid line), $\alpha = \pi/4$ (dotted line), and the c-axis of the crystal along the x-direction (dot-dashed line). Here $h_0/E_F = 0.05$ is taken.

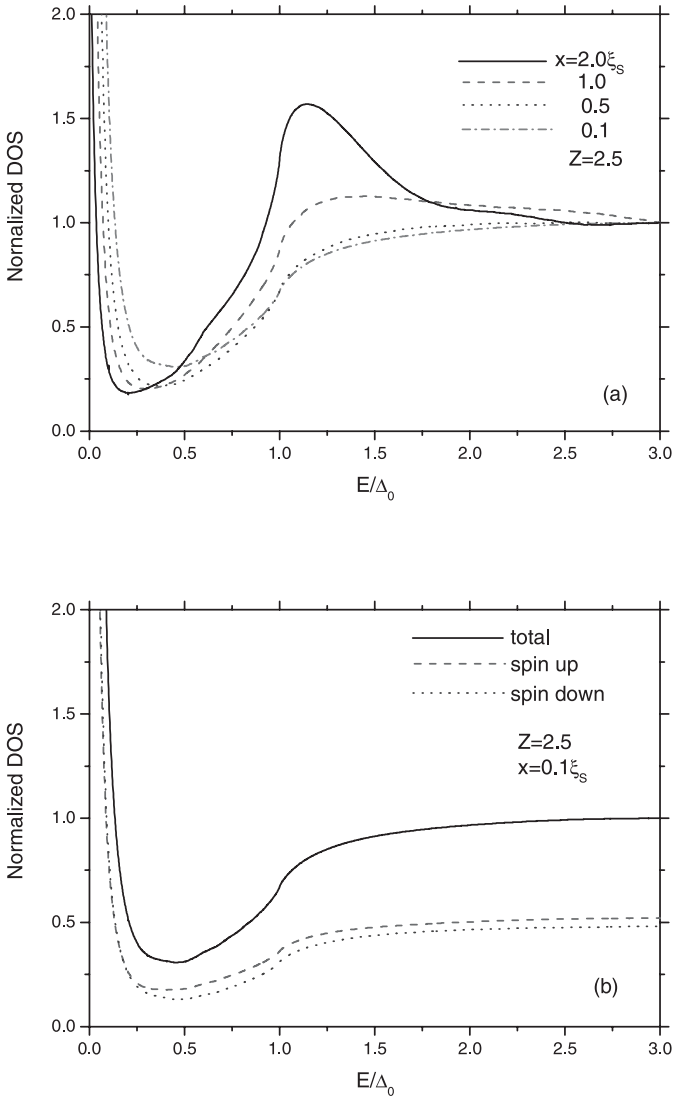

Fig. 3. (a) Local DOS in SC at $x/\xi_S = 0.1$, 0.5, 1.0, and 2.0. (b) local DOS with spin up and down (dashed and dotted lines) and total (solid line) in SC at $x/\xi_S = 0.1$. Here $\alpha = \pi/4$, $h_0/E_F = 0.05$, and $Z = 2.5$.

$\alpha = \pi/4$ is the oscillation periods of $F(x)$ in FM. The oscillation period for $\alpha = 0$ is close to $2\pi\xi_F$, while that for $\alpha = \pi/4$ is significantly shorter. This difference may be understood by the following argument. As shown in equations (8) and (13), the oscillation period L of $F(x)$ in FM is determined by $(q_{e\uparrow}\cos\theta - q_{h\downarrow}\cos\theta_A)L = 2\pi$ as well as the integral over θ. For $\alpha = 0$, the normal injection ($\theta = \theta_A = 0$) dominates the integral over θ and so $L = 2\pi/(q_{e\uparrow} - q_{h\downarrow}) = 2\pi\xi_F$, the same as that in the s-wave SC case [19]. For $\alpha = \pi/4$, the normal injection of $\theta = 0$ that comes from the node of $F(x)$ is of not importance, and what plays a dominant role in $F(x)$ in FM is the injection for θ below but close to $\pm\pi/4$. It is easily shown that the absolute value of $q_{e\uparrow}\cos\theta - q_{h\downarrow}\cos\theta_A$ is always greater than that for $\theta = \theta_A = 0$ provided that the condition $q_{e\uparrow}\sin\theta = q_{h\downarrow}\sin\theta_A$ is taken into account. As a result, the period for $\alpha = \pi/4$ is shorter than that for $\alpha = 0$. For the c-axis of the crystal along the x-direction, the period is also given by $L = 2\pi\xi_F$, the same as that in $\alpha = 0$ for the reason given above. In this case, the proximity effect is stronger than that for $\alpha = 0$ but weaker than for $\alpha = \pi/4$, corresponding seemingly to an average result.

Figure 3a shows the normalized local-DOS $N(x, E)$ of quasiparticles in SC for $\alpha = \pi/4$. We see that the DOS has a sharp peak at $E = 0$; with increasing distance from the interface, the zero-energy peak is gradually lowered and becomes narrow, and the shape of $N(x, E)$ tends toward that of the bulk d-wave SC, with $\xi_S = \hbar v_F/2\Delta_0$ the coherence length in SC. More interestingly, the DOS in SC is found to be spin dependent, as shown in Figure 3b. From different DOS for spin-up and spin-down quasiparticles, it follows that a weak ferromagnetism appears in SC

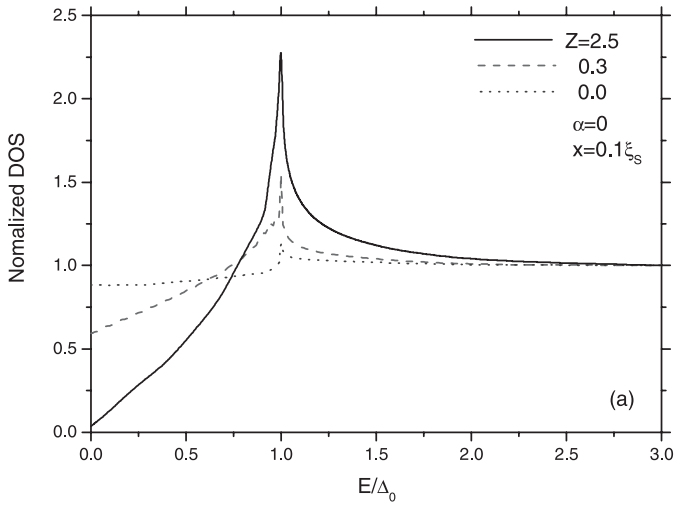

Fig. 4. Local DOS in SC at $x/\xi_S = 0.1$ for $Z = 2.5$ (solid line), 0.3 (dashed line), and 0 (dotted line). Here $\alpha = 0$ and $h_0/E_F = 0.05$.

near the interface, which arises from the injection of spin-polarized electrons from FM to SC. There is a coexistence of superconductivity and ferromagnetism in the local region near the FM/SC interface. This result is consistent with that obtained in a recent work [42]. In Figure 4 we plot $N(x = 0.1\xi_S, E)$ in SC for $\alpha = 0$ with different Z. For large Z the proximity effect is weak and the local DOS is close to that in the bulk d-wave SC for $\alpha = 0$. With decreasing Z, the enhanced proximity effect causes the DOS at $E = 0$ to increase and its peak at $E = \Delta_0$ to lower. Different DOS shapes in SC for $\alpha = \pi/4$ and 0, respectively, as shown in Figures 3a and 4, stem from the anisotropy of the superconducting order parameter in the d-wave SC.

Figure 5 shows the normalized DOS in FM versus energy E/Δ_0 for $\alpha = \pi/4$ with different Z. It is found that there are two types of SC-induced DOS with different shapes, superimposed on the DOS background in FM. For example, at $x = -0.5\xi_F$ the DOS displays a sharp peak at $E = 0$, as shown in Figures 5a and 5c, while at $x = -0.75\xi_F$, there is an inversion in shape of the SC-induced DOS, as shown in Figures 5b and 5d. Both of them arise from the interference effect of the spin-σ electrons and the Andreev reflected holes with spin-$\bar{\sigma}$. It is expected that these two types of DOS in FM would be observed in future experiments, e.g., a tunneling spectrum measurement on a normal-metal/I/$La_{1-x}Sr_xMnO_3$/$YBa_2Cu_3O_7$ structure where I stands for a thin insulating layer. Such an SC-induced DOS will disappear gradually with distance from the interface.

4 Summary

We have applied the Nambu spinor Green's function approach and BTK theory to study the proximity effect in FM/d-wave SC junctions. It is found that, unlike in the s-wave case, the magnitude of the proximity effect for the d-wave SC depends to a great extent on the orientation of the crystal with respect to the interface normal, being strongest for $\alpha = \pi/4$ and weakest for $\alpha = 0$. On the FM side, the superconducting order parameter induced by the proximity effect has a change from "0 state" to "π state" as the distance from the interface increases. The injection of the Cooper pairs from the d-wave SC leads to two types of different DOS shapes with d-wave superconducting features. On the SC side, the injection of spin-polarized electrons from FM induces the spin dependence of DOS near the interface and so the local coexistence of weak ferromagnetism and d-wave superconductivity.

This work was supported by National Natural Science Foundation of China under Grant No. 10174011 and 10374046, and also by the Jiangsu Province Natural Science Foundation of China under Grant No. BK2001002.

Appendix A: Expressions for reflection and transmission coefficients in Green's functions

Using the boundary conditions on the wave functions and carrying out a little tedious algebra, we find

$$a_1^{\bar{\sigma}} = 2q_e^{\sigma}\cos\theta(k_+^d\cos\theta_S + k_-^d\cos\theta_S)u_-^d v_+^d/A,$$

$$\begin{aligned} b_1^{\sigma} = {} & [(q_e^{\sigma}\cos\theta - k_+^d\cos\theta_S - 2ik_F\cos\theta Z) \\ & \times (k_-^d\cos\theta_S + q_h^{\bar{\sigma}}\cos\theta_A - 2ik_F\cos\theta Z)u_+^d u_-^d e^{i\phi_+^d} \\ & + (k_+^d\cos\theta_S - q_h^{\bar{\sigma}}\cos\theta_A + 2ik_F\cos\theta Z) \\ & \times (k_-^d\cos\theta_S + q_e^{\sigma}\cos\theta - 2ik_F\cos\theta Z)v_+^d v_-^d e^{i\phi_-^d}]/A, \end{aligned}$$

$$a_2^{\sigma} = 2q_h^{\bar{\sigma}}\cos\theta_A(k_+^d\cos\theta_S + k_-^d\cos\theta_S)u_+^d v_-^d e^{i(\phi_+^d+\phi_-^d)}/A,$$

$$\begin{aligned} b_2^{\bar{\sigma}} = {} & [(q_h^{\bar{\sigma}}\cos\theta_A - k_-^d\cos\theta_S + 2ik_F\cos\theta Z) \\ & \times (k_+^d\cos\theta_S + q_e^{\sigma}\cos\theta + 2ik_F\cos\theta Z)u_+^d u_-^d e^{i\phi_+^d} \\ & + (k_-^d\cos\theta_S - q_e^{\sigma}\cos\theta - 2ik_F\cos\theta Z) \\ & \times (k_+^d\cos\theta_S + q_h^{\bar{\sigma}}\cos\theta_A + 2ik_F\cos\theta Z)v_+^d v_-^d e^{i\phi_-^d}]/A, \end{aligned}$$

$$\begin{aligned} a_3^{\bar{\sigma}} = {} & [(q_e^{\sigma}\cos\theta - \tilde{k_-^d}\cos\theta_S - 2ik_F\cos\theta Z) \\ & \times (k_+^d\cos\theta_S - q_h^{\bar{\sigma}}\cos\theta_A - 2ik_F\cos\theta Z)u_-^d v_+^d e^{i\phi_-^d} \\ & + (q_h^{\bar{\sigma}}\cos\theta_A + \tilde{k_-^d}\cos\theta_S + 2ik_F\cos\theta Z) \\ & \times (k_+^d\cos\theta_S + q_e^{\sigma}\cos\theta - 2ik_F\cos\theta Z)u_+^d v_-^d e^{i\phi_+^d}]/B, \end{aligned}$$

$$\begin{aligned} b_3^{\sigma} = {} & [(k_-^d\cos\theta_S - q_e^{\sigma}\cos\theta + 2ik_F\cos\theta Z) \\ & \times (q_h^{\bar{\sigma}}\cos\theta_A + \tilde{k_-^d}\cos\theta_S + 2ik_F\cos\theta Z)(v_-^d)^2 e^{i\phi_-^d} \\ & + (q_h^{\bar{\sigma}}\cos\theta_A + k_-^d\cos\theta_S + 2ik_F\cos\theta Z) \\ & \times (q_e^{\sigma}\cos\theta - \tilde{k_-^d}\cos\theta_S - 2ik_F\cos\theta Z)(u_-^d)^2 e^{i\phi_-^d}]/B, \end{aligned}$$

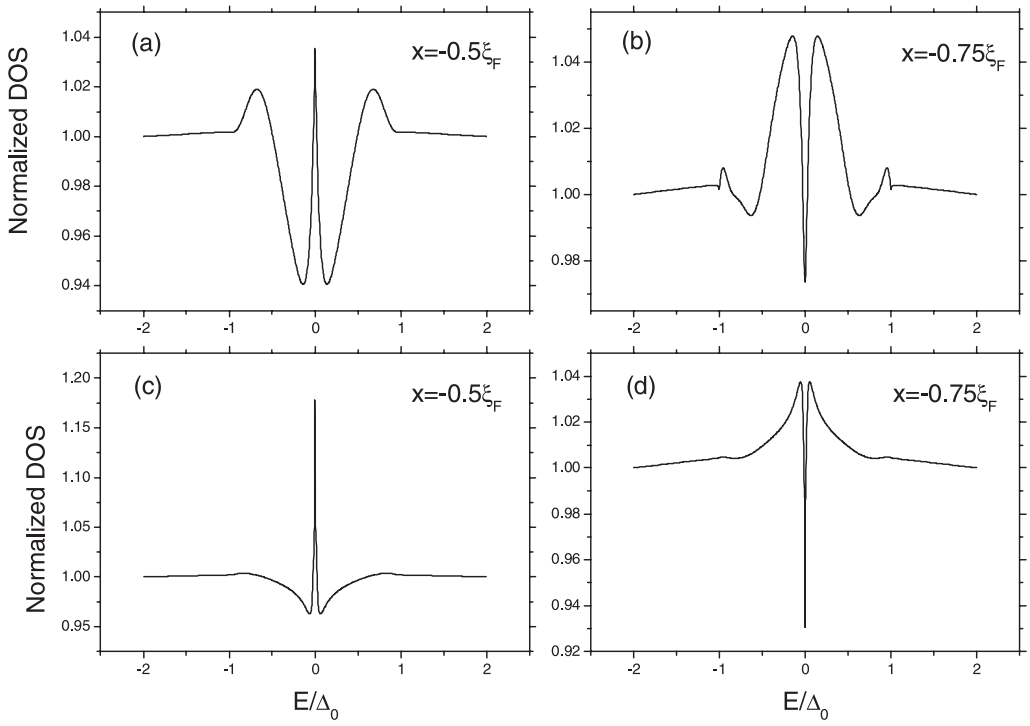

Fig. 5. Local DOS in FM at $x/\xi_F = -0.5$ and -0.75 for different $Z = 0.3$ (a, b) and 2.5 (c, d).

$$
\begin{aligned}
a_4^{\sigma} = [&(\tilde{k_+^d}\cos\theta_S + q_e^{\sigma}\cos\theta - 2ik_F\cos\theta Z)\\
&\times (k_-^d\cos\theta_S + q_h^{\bar\sigma}\cos\theta_A + 2ik_F\cos\theta Z)u_-^d v_+^d e^{i\phi_+^d}\\
&-(\tilde{k_+^d}\cos\theta_S - q_h^{\bar\sigma}\cos\theta_A - 2ik_F\cos\theta Z)\\
&\times (k_-^d\cos\theta_S - q_e^{\sigma}\cos\theta + 2ik_F\cos\theta Z)u_+^d v_-^d e^{i\phi_-^d}]/B,
\end{aligned}
$$

and

$$
\begin{aligned}
b_4^{\bar\sigma} = [&(q_h^{\bar\sigma}\cos\theta_A - \tilde{k_+^d}\cos\theta_S + 2ik_F\cos\theta Z)\\
&\times (k_+^d\cos\theta_S + q_e^{\sigma}\cos\theta - 2ik_F\cos\theta Z)(u_+^d)^2 e^{i\phi_+^d}\\
&+(\tilde{k_+^d}\cos\theta_S + q_e^{\sigma}\cos\theta - 2ik_F\cos\theta Z)\\
&\times (k_+^d\cos\theta_S - q_h^{\bar\sigma}\cos\theta_A - 2ik_F\cos\theta Z)(v_+^d)^2 e^{i\phi_+^d}]/B,
\end{aligned}
$$

with

$$
\begin{aligned}
A = &(q_e^{\sigma}\cos\theta + k_+^d\cos\theta_S + 2ik_F\cos\theta Z)\\
&\times (k_-^d\cos\theta_S + q_h^{\bar\sigma}\cos\theta_A - 2ik_F\cos\theta Z)u_+^d u_-^d e^{i\phi_+^d}\\
&+(q_h^{\bar\sigma}\cos\theta_A - k_+^d\cos\theta_S - 2ik_F\cos\theta Z)\\
&\times (k_-^d\cos\theta_S - q_e^{\sigma}\cos\theta - 2ik_F\cos\theta Z)v_+^d v_-^d e^{i\phi_-^d},
\end{aligned}
$$

and

$$
\begin{aligned}
B = &(k_-^d\cos\theta_S - q_e^{\sigma}\cos\theta + 2ik_F\cos\theta Z)\\
&\times (k_+^d\cos\theta_S - q_h^{\bar\sigma}\cos\theta_A - 2ik_F\cos\theta Z)v_+^d v_-^d e^{i\phi_-^d}\\
&-(q_h^{\bar\sigma}\cos\theta_A + k_-^d\cos\theta_S + 2ik_F\cos\theta Z)\\
&\times (k_+^d\cos\theta_S + q_e^{\sigma}\cos\theta - 2ik_F\cos\theta Z)u_+^d u_-^d e^{i\phi_+^d}.
\end{aligned}
$$

References

1. Z. Radovic, M. Ledvij, L. Dobrosavljevic-Grujic, A.I. Buzdin, J.R. Clem, Phys. Rev. B **44**, 759 (1991)
2. Y. Tanaka, S. Kashiwaya, Phys. Rev. Lett. **74**, 3451 (1995)
3. J.Q. Xiao, C.L. Chien, Phys. Rev. Lett. **76**, 1727 (1996)
4. E.A. Demler, G.B. Arnold, M.R. Beasley, Phys. Rev. B **55**, 15174 (1997)
5. S. Kashiwaya, Y. Tanaka, N. Yoshida, M.R. Beasley, Phys. Rev. B **60**, 3572 (1999)
6. J.X. Zhu, B. Friedman, C. S. Ting, Phys. Rev. B **59**, 9558 (1999)
7. J.X. Zhu, C.S. Ting, Phys. Rev. B **61**, 1456 (2000)
8. L. Lazar, K. Westerholt, H. Zabel, L.R. Tagirov, Yu.V. Goryunov, N.N. Garif'yanov, I.A. Garifullin, Phys. Rev. B **61**, 3711 (2000)
9. S. Kashiwaya, Y. Tanaka, Rep. Prog. Phys. **63**, 1641 (2000)
10. T. Kontos, M. Aprili, J. Lesueur, X. Grison, Phys. Rev. Lett. **86**, 304 (2001)
11. M. Zareyan, W. Belzig, Yu.V. Nazarov, Phys. Rev. Lett. **86**, 308 (2001)
12. V.V. Ryazanov, V.A. Oboznov, A.Yu. Rusanov, A.V. Veretennikov, A.A. Golubov, J. Aarts, Phys. Rev. Lett. **86**, 2427 (2001)
13. Z.C. Dong, D.Y. Xing, Z.D. Wang, Z.M. Zheng, J.M. Dong, Phys. Rev. B **63**, 144520 (2001)
14. F.S. Bergeret, A.F. Volkov, K.B. Efetov, Phys. Rev. Lett. **86**, 4096 (2001)
15. J. Aumentado, V. Chandrasekhar, Phys. Rev. B **64**, 54505 (2001)
16. E. Vecino, A. Martín-Rodero, A. Levy Yeyati, Phys. Rev. B **64**, 184502 (2001)
17. I. Baladié, A. Buzdin, Phys. Rev. B **64**, 224514 (2001)
18. K. Halterman, O.T. Valls, Phys. Rev. B **65**, 14509 (2001)

19. G.Y. Sun, D.Y. Xing, J.M. Dong, M. Liu, Phys. Rev. B **65**, 174508 (2002); G.Y. Sun, D.Y. Xing, R. Shen, H.Q. Lin, Eur. Phys. J. B **30**, 33 (2002)
20. K. Halterman, O.T. Valls, Phys. Rev. B **66**, 224516 (2002)
21. A. Kohen, G. Leibovitch, G. Deutscher, Phys. Rev. Lett. **90**, 207005 (2003)
22. A. Bagrets, C. Lacroix, A. Vedyayev, Phys. Rev. B **68**, 54532 (2003).
23. O. Bourgeois, A. Frydman, R.C. Dynes, Phys. Rev. B **68**, 92509 (2003)
24. A.F. Andreev, Phys. JEPT **19**, 128 (1964)
25. C.R. Hu, Phys. Rev. Lett. **72**, 1526 (1994)
26. N. Stefanakis, R. Melin, J. Phys.: Condens. Matter **15**, 3401 (2003)
27. A.A. Abrikosov, *Fundamentals of the Theory of Metals* (North-Holland, Amstergam, 1988)
28. K. Yang, S.L. Sondhi, Phys. Rev. B **57**, 8566 (1998)
29. P. Fulde, A. Ferrel, Phys. Rev. **135**, A550 (1964)
30. A. Larkin, Y. Ovchinnikov, Sov. Phys. JETP **20**, 762 (1965)
31. N.I. Karchev, K.B. Blagoev, K.S. Bedell, P.B. Littlewood, Phys. Rev. Lett. **86**, 846 (2001)
32. R. Shen, Z.M. Zheng, S. Liu, D.Y. Xing, Phys. Rev. B **67**, 24514 (2003)
33. M. Cuoco, P. Gentile, C. Noce, Phys. Rev. Lett. **91**, 197003 (2003)
34. B.R. Zhao, X.L. Dong, P.S. Luo, Z.X. Zhao, L.M. Peng, Y.M. Ni, X.G. Qiu, S. Awaaji, K. Watanabe, F. Wu, B. Xu, L.H. Zhao, F.C. Zhang, Eur. Phys. J. B **25**, 19 (2002)
35. G. Jakob, V.V. Moshchalkov, Y. Bruynseraede, Appl. Phys. Lett. **66**, 2564 (1995)
36. G.E. Blonder, M. Tinkham, T.M. Klapwijk, Phys. Rev. B **25**, 4515 (1982)
37. W.L. McMillan, Phys. Rev. **175**, 559 (1968)
38. P.G. de Gennes, *superconductivity of Metals and Alloys* (Benjamin, New York, 1966)
39. Y. Nambu, Phys. Rev. **117**, 648 (1960)
40. A. Furusaki, H. Takayanagi, M.Tsukada, Phys. Rev. B **45**, 10563 (1992)
41. M. Liu, D.Y. Xing, Z.D. Wang, Phys. Rev. B **55**, 3181 (1997)
42. F.S. Bergeret, A.F. Volkov, K.B. Efetov, `arXiv:cond-mat/0307468`